Theoretical Studies of Competitive Gas-Phase S_N2 and E2 Reactions of $NCCH_2CH_2Cl$ with OH^- and SH^-

Dong Soo Chung, Chang Kon Kim, Bon-Su Lee, and Ikchoon Lee*

Department of Chemistry, Inha University, Inchon, 402-751, Korea

Received: March 18, 1997; In Final Form: May 30, 1997[⊗]

The gas-phase reactions of OH^- and SH^- with $NCCH_2CH_2Cl$ have been studied with ab initio methods using the 6-31+G* basis sets. The electron correlation effect was accounted for at the MP2 level of theory. Both the S_N2 and E2(anti) reactions are exothermic and have negative activation barriers when Cl^- is the leaving group. Overall, E2 is preferred to S_N2, and E2(anti) is favored over E2(gauche) for both OH^- and SH^-, indicating the preference of an antiperiplanar transition state in the gas phase. Since SH^- is a weaker gas-phase nucleophile than OH^-, the transition state occurs later on the reaction coordinate. The results of this work are consistent with those of gas-phase experimental studies which indicated that first-row nucleophiles undergo both S_N2 and E2 reactions, whereas second-row nucleophiles have lower abilities to induce elimination reactions. Substitution of a CN group for a β-hydrogen of CH_3CH_2Cl to $NCCH_2CH_2Cl$ is found to enhance both the S_N2 and E2 reactivities and makes the β-H-elimination become more E1cb-like. Incorporation of the electron correlation effect at higher levels, MP3, MP4D, MP4DQ, and MP4SDQ, gives essentially the same order of reactivities as found at the MP2 level, except the preference of S_N2 over E2(anti) with SH^- at the higher level of theory.

I. Introduction

The S_N2 and E2 reactions are the two important types of reactions in organic chemistry that have been the subjects of extensive studies for many years.[1,2] Experimental studies in solution have led to a number of regularities relating the reactivity to the nature and structure of the nucleophile or the bases, the leaving group, and the substrate. Results of these solution-phase studies are, however, masked by solvent and ion-pairing effects, and no unambiguous information can be obtained from this source about the "intrinsic" properties under a solvent-free environment. In this respect theoretical and gas-phase studies provide two of the most useful and important approaches to a probing mechanism. Recently, S_N2 and E2 reactions have been studied in the gas phase using ion cyclotron resonance, flowing afterglow, and mass spectrometric techniques.[3,4] Gas-phase studies on the nucleophilic substitution reactions over the past decade have provided some important information promoting the understanding of the intrinsic issues involved. The general double-well character of the potential energy surface has been verified.[3o] Involvement of a tetrahedral structure in the acyl transfer reactions has been shown.[5] The concept of intrinsic nucleophilicity for reaction at a carbon center has been developed,[3h] and the effects of reaction exothermicity in terms of rate−equilibrium relationships have been described.[3g,6] Insights into the effects of substrate structure on the gas-phase S_N2 reactivity have been provided.[3q] Reports of gas-phase experimental studies on E2 reactions are relatively scarce, and in most cases are carried out under competitive conditions with S_N2 pathways.[3m,n,4] Results indicated that strongly basic localized anions containing F, N, or O at the nucleophilic center react by preferential E2 reaction; in contrast, delocalized carbanions react by displacement.[4b] Sulfur anions (RS^-) are shown to induce elimination much less readily than do oxy anions (RO^-) even when the two anions have identical basicities.[3m]

The S_N2 reaction is probably the most thoroughly studied and analyzed reaction in theoretical organic chemistry.[1c,d,7] In contrast, relatively little theoretical work has been reported on the E2 reaction.[8] Gronert reported results of ab initio studies of the gas-phase reactions of F^- and PH_2^- with CH_3CH_2Cl,[8d] and F^- with $(CH_3)_2CHCl$ and $CH_3CH_2CH_2Cl$.[8f] E2 as well S_N2 pathways were investigated and concluded that (i) first-row nucleophiles are well-suited for both S_N2 and E2 reactions, whereas second-row nucleophiles are more limited to S_N2 reactions; (ii) the addition of a CH_3 group at the α-carbon increases the S_N2 barrier, whereas that at the β-carbon reduces the barrier, and CH_3 groups in both cases stabilize the E2 transition state (TS); and (iii) stereochemically in both systems anti (periplanar) rather than syn elimination is preferred.[3d,f]

SCHEME 1

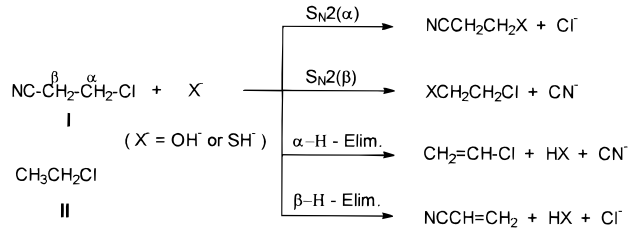

In this work, to gain further insights into the details of gas-phase S_N2−E2 competitive reactions, we carried out ab initio studies on the reactions of $NCCH_2CH_2Cl$, **I**, with OH^- and SH^-, with particular emphasis on the effects of a strongly electron withdrawing substituent, CN, on the reactivity and TS structures.

In the present work, four competitive reaction pathways, Scheme 1, are considered with various stereochemical preferences for the elimination TSs, i.e., syn, anti, or gauche conformation.

Calculations

Calculations were carried out using the Gaussian 92 program package.[9] All structures were fully optimized using the 6-31+G* basis set.[10] In addition the MP2/6-31+G*[10] optimizations were carried out with the frozen-core approximation. Harmonic vibrational frequencies were calculated at the RHF/

[⊗] Abstract published in *Advance ACS Abstracts,* November 1, 1997.

S1089-5639(97)00975-4 CCC: $14.00 © 1997 American Chemical Society

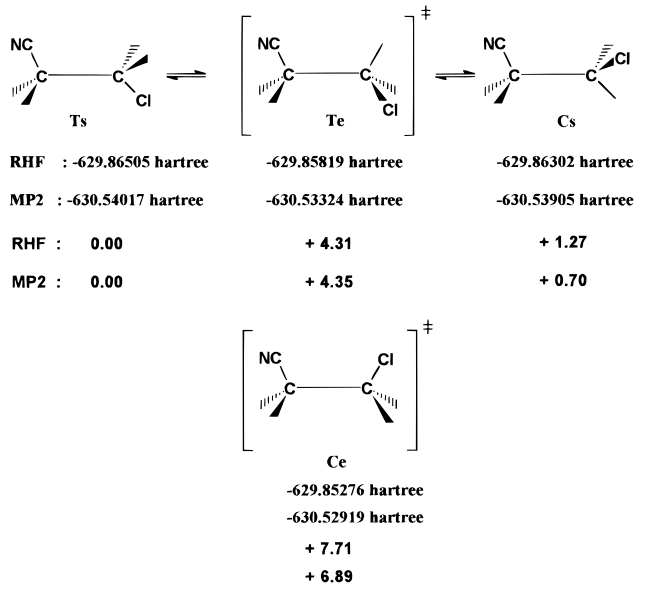

Figure 1. Calculated electronic energies of substrates at the RHF and MP2 levels.

TABLE 1: Electronic Energies (*E*) and Proton Affinities (PA) of Nucleophiles, X^-

X^-	level	*E* (hartree)	PA (kcal mol^{-1})	expt[a] (kcal mol^{-1})
OH^-	RHF/6-31+G*	−75.376 42	402.4	390.8
	MP2/6-31+G*	−75.588 36	389.9	
SH^-	RHF/6-31+G*	−398.106 89	352.2	351.2
	MP2/6-31+G*	−398.229 61	351.8	

[a] Reference 4b.

6-31+G* and MP2/6-31+G* levels, and all stationary points on the potential energy surfaces were characterized by confirming all positive and only one imaginary vibrational frequencies (for TS).[11] Additional single-point calculations based on the MP2 optimized geometries were carried out at the MP3, MP4D, MP4DQ, and MP4SDQ levels.[10] For comparison, we have also carried out RHF and MP2 calculations on ethyl chloride, **II**.

Results and Discussion

S_N2 Reactions. *Reactants and Reactant Complexes*. The substrate, 2-cyanoethyl chloride ($NCCH_2CH_2Cl$), **I**, has two stable rotamers, cis-staggered (cs) and trans-staggered (ts), and between them there are two types of rotational barriers corresponding to the two eclipsed rotamers, trans-eclipsed (te) and cis-eclipsed (ce), as shown in Figure 1.

The ts rotamer is marginally more stable (by 0.7 kcal mol^{-1} at the MP2 level) than the cs form and the rotation through the te form should be more facile than through the ce form (4.4 vs 6.9 kcal mol^{-1} at the MP2 level). The rotational barrier is higher only by 1.5 kcal mol^{-1} than that within ethane (2.9 kcal mol^{-1}),[12] and relatively free rotation should be possible. Since the stabilities of the two rotamers are not significantly different, there will be an equilibrium state of the two rotamers, ts and cs. However we considered that reactions proceeded from the more stable ts form to the subsequent steps in the reaction pathway.

To test the performance of the basis set and level of theory adopted, the gas-phase proton affinities (PA) of OH^- and SH^- were calculated and compared to experimental values.[4b] The results in Table 1 show that the MP2 values are in good agreement with the corresponding experimental values (within 1.0 kcal mol^{-1}). The incorporation of electron correlation effects (MP2) leads to the improvement of the calculated PAs, and the results clearly indicate that the present level of theory is adequate. The PA of OH^- is higher by ca. 20 kcal mol^{-1}, whereas SH^- is lower by a similar amount than the PAs of F^- and PH_2^- (371.5 and 370.9 kcal mol^{-1}), which were used as anionic base nucleophiles in the theoretical studies of reactions with ethyl chloride, **II**, by Gronert.[8d]

TABLE 2: Calculated Electronic Energies (*E*/hartree) and Frequencies for the Lowest Vibrational Modes (ν/cm^{-1}) of the Reactant Complexes (RC) at RHF/6-31+G* Level

X^-		RC1	RC2	RC3
OH^-	*E*	−705.270 35	−705.272 23	−705.289 55
	ν	81.98i[a]	120.06i[a]	56.97
SH^-	*E*	−1027.985 02	−1027.987 31	−1027.998 38
	ν	73.79i[a]	59.42i[a]	35.27

[a] Imaginary frequency.

SCHEME 2

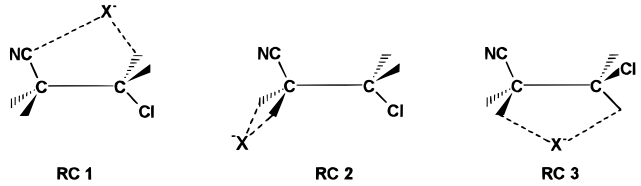

In the gas phase, the first energy minimum along the reaction coordinate is a weakly bound ion−dipole complex formed between the two reactants, an anionic nucleophile and substrate, i.e., a reactant complex (RC). Since in the present reaction system two rotamers, ts and cs, have equivalent stability and relative population, three types of RCs shown in Scheme 2 are conceivable: RC1 and RC2 are the most likely forms leading to $S_N2(\alpha)$ and β-H-elimination reactions, respectively, whereas all four reaction pathways in Scheme 1 are possible from RC3. The electronic energies and harmonic frequencies of the lowest vibrational modes for the three ion−dipole complexes are presented in Table 2. We note that RC1 and RC2 each have an imaginary frequency, indicating that they are not stable stationary points. In fact both of these complexes correspond to transition states on the pathways leading to the only possible complex, RC3, which is also the most stable complex. The MP2 structures of the two RC3 complexes (with OH^- and SH^-) are shown in Figure 2.

Thus, even though two stable substrate rotamers of equivalent stability exist, only one reactant complex, RC3, is formed. The MP2 structures in Figure 2 show that distances between OH^- and the β-hydrogen and α-carbon are 1.791 and 2.850 Å, respectively, whereas those for SH^- are 2.576 and 3.527 Å. The reactant complex with SH^- is consequently looser and more weakly bound than that with OH^-, and hence the stabilization energy ($\Delta E_{RC} = -20.71$ kcal mol^{-1}) is lower by ($\delta\Delta E_{RC} =$) 11.9 kcal mol^{-1} than that with OH^- ($\Delta E_{RC} = -32.57$ kcal mol^{-1} at the MP2 level). This difference in the stabilization energy between the first- and second-row nucleophilic center is rather larger than that found by Gronert[8d] for the S_N2 reactions of F^- and PH_2^- with ethyl chloride, **II** ($F^-/PH_2^- \rightarrow \delta\Delta E_{RC} = 15 - 8 = 7$ kcal mol^{-1}). This may be caused by the large difference in the PA between OH^- and SH^- and also by a stronger hydrogen bond formation between the anionic nucleophile and a β-hydrogen which has an increased acidity due to a strong electron-withdrawing group, CN, on the β-carbon in the present reaction system. This is evident from a shorter $X^-\cdots H_\beta$ distance than $X^-\cdots H_\alpha$ in both reactant complexes in Figure 2.

S_N2 Transition States. The generalized potential energy surface for an exothermic S_N2 displacement reaction in the gas

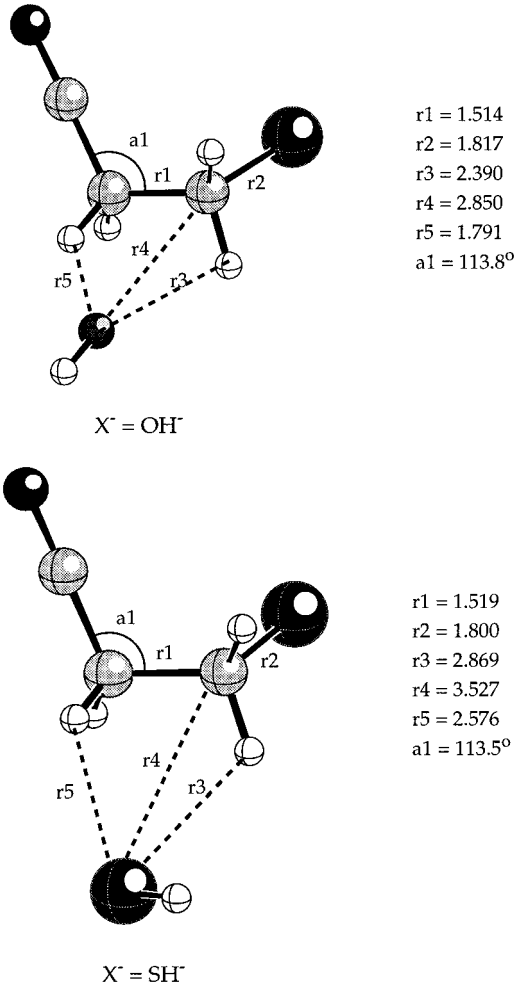

Figure 2. Structures of reactant complexes at the MP2 level (bond lengths in angstroms.)

SCHEME 3

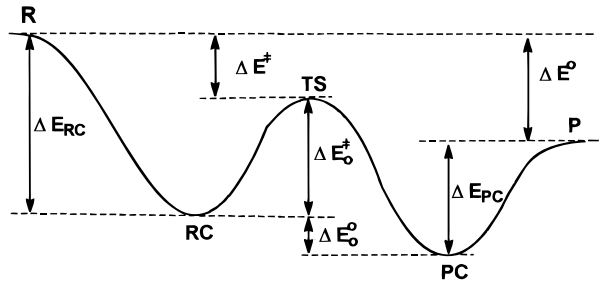

phase is presented in Scheme 3, where various quantities of energetics are defined. For example, $\Delta E_0^{\ddagger}$ and $\Delta E^{\ddagger}$ are the two barrier heights measured from the reactant complex, RC, level (a central barrier) and from the separated reactants level (an activation energy). The calculated values of energetics involved in the S_N2 reactions are summarized in Table 3. Reference to Table 3 reveals that in general a stronger nucleophile, OH^-, leads to lower activation barriers ($\Delta E^{\ddagger}$) as well as central barriers ($\Delta E_0^{\ddagger}$) compared to a weaker nucleophile, SH^-. The reactions with OH^- are more favorable both kinetically ($\delta\Delta E_{MP}^{\ddagger} \cong 20$ kcal mol^{-1}) and thermodynamically ($\delta\Delta E_{MP}^{\circ} \cong 30$ kcal mol^{-1}) compared to those with SH^-. These results are consistent with the experimentally observed weak nucleophilicity of sulfur nucleophiles in the gas phase,[3m] which is in contrast to the extraordinary nucleophilicity observed in solution, most probably due to a solvent effect.[3f] The $\delta\Delta E_{MP}^{\ddagger}$ ($=\Delta E^{\ddagger}(SH^-) - \Delta E^{\ddagger}(OH^-)$) of ca. 20 kcal mol^{-1} for the reactions of **I** is higher

TABLE 3: Calculated Activation Energies ($\Delta E^{\ddagger}$ and $\Delta E_0^{\ddagger}$), Complexation Energies (ΔE_{RC} and ΔE_{PC}), and Reaction Energies (ΔE° and ΔE_0°) for the S_N2 Reaction Paths in kcal mol^{-1}

X^-	Z^a	level	$\Delta E^{\ddagger}$	$\Delta E_0^{\ddagger}$	ΔE_{RC}	ΔE_{PC}	ΔE°	ΔE_0°
OH^-	Cl	RHF	−21.22 (−12.35)[b]	8.95	−30.17	−13.72	−72.67	−56.22
		MP2	−21.14 (−10.27)[b]	11.44	−32.57	−17.28	−53.83	−38.54
SH^-	Cl	RHF	2.30 (6.50)[b]	18.89	−16.60	−17.93	−24.12	−25.45
		MP2	−2.54 (5.48)[b]	18.18	−20.71	−23.33	−24.12	−26.73
OH^-	CN	RHF	11.77	41.94	−30.17	−10.64	−36.58	−18.94
		MP2	9.66	42.24	−32.57	−13.63	−23.20	−4.25
SH^-	CN	RHF	38.19	54.78	−16.60	−11.95	11.68	16.33
		MP2	29.04	49.76	−20.71	−13.76	6.52	13.47

[a] Leaving group. [b] Values in parentheses are the activation energies for reactions of CH_3CH_2Cl with X^-.

than the corresponding value of ca. 15 kcal mol^{-1} for the reaction of **II**. Thus substitution of a strong electron acceptor, CN, for a β-hydrogen leads to a greater lowering of $\Delta E^{\ddagger}$ for the reaction with a stronger nucleophile, OH^-. For the reactions of **II** with nucleophiles having similar PAs, F^- (371.5 ± 0.2 kcal mol^{-1}) and PH_2^- (370.9 ± 2.0 kcal mol^{-1}), $\delta\Delta E_{MP}^{\ddagger}$ ($=\Delta E^{\ddagger}(PH_2^-) - \Delta E^{\ddagger}(F^-)$) is even smaller, ca. 10 kcal mol^{-1}.[8d] This comparison shows that the activation energies, $\Delta E^{\ddagger}$, for the first- and second-row nucleophiles, diverge to a greater extent with the greater difference in the nucleophilicty and as the substrate becomes more electron accepting.

The reactions with the Cl^- leaving group, i.e., $S_N2(\alpha)$ reactions, are exothermic and have negative activation energies in both nucleophiles, OH^- and SH^-. The reactions can therefore proceed in the gas phase, but the central barriers for the reaction of the SH^- nucleophile are relatively high compared to those of the OH^- nucleophile. Thus the rate for the reaction of the SH^- nucleophile may be slow with low reaction efficiency compared with the reactions of the OH^- nucleophile. Incorporation of electron correlation effects at the MP2 level seems to have relatively little effect on the barrier heights; for the stronger nucleophile, OH^-, the barriers are elevated ($\Delta E^{\ddagger}$ and $\Delta E_0^{\ddagger}$ are raised by 0.1 and 2.5 kcal mol^{-1} respectively), whereas they are lowered (by 4.8 and 0.8 kcal mol^{-1}, respectively) for the weaker nucleophile, SH^-. A similar behavior was obtained for the activation barriers to the S_N2 reactions of ethyl chloride, **II**, shown in Table 3. It has been suggested that the activation energy lowering incurred by inclusion of electron correlation effects arises from a greater contribution of a more electron-localized configuration, **III**, to the TS, which leads to a larger magnitude of electron correlation energy in the TS than in the reactant.[13,7l] In structure **III**, X^- and Z^- represent the

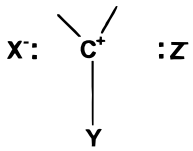

III

nucleophile and leaving group, and Y denotes a substituent on the substrate. In our reaction system, $X^- = OH^-$ or SH^-, $Z^- = Cl^-$, and $Y = CH_2CN$. The decrease in the correlated activation energy was found to be greater with more electronegative X, Y, and/or Z groups.[3p,7n,o] Since SH^- forms a looser TS than OH^- (vide infra), it appears that in the reactions with

TABLE 4: Calculated %CX‡, %CZ‡, %L‡, and Bond Orders, *n*, in the TS of S_N2 Reactions at the MP2 Level

path	X^-	Z	%CX‡	%CZ‡	%L‡	$n_{(C-X)}$	$n_{(C-Z)}$
$S_N2(\alpha)$	OH^-	Cl	24.9	37.5	62.4	0.31	0.55
	SH^-	Cl	28.7	37.6	66.3	0.32	0.48
$S_N2(\beta)$	OH^-	CN	27.9	46.3	74.2	0.40	0.41
	SH^-	CN	30.4	37.8	68.2	0.39	0.35

SH^- there is a greater tendency of forming a more electron-localized TS, like **III**. These interpretations are supported by looseness of the TS,[1c] defined by %L‡ = %CX‡ + %CZ‡ and %CX‡(or %CZ‡) = 100 ($d^‡ - d^o$)/d^o, where $d^‡$ and d^o denote bond lengths in the TSs and ion−dipole complexes, RC for %CX‡, and PC for %CZ‡, respectively. A large %L‡ is a characteristic of a looser TS structure. These values are collected in Table 4. Reference to Table 4 shows that %L‡ values are 62.4 for OH^- and 66.3 for SH^-, respectively.

The reaction paths in which CN^- is a leaving group, i.e., $S_N2(\beta)$ reactions, have high energy barriers, $\Delta E^‡$ and $\Delta E_0^‡$, due to poor leaving ability of CN^-, and in addition for SH^- the reaction is endothermic. The inclusion of electron correlation at the MP2 level reduces the barrier heights. However, high energy barriers and endothermic nature (for SH^-) of the reaction predict that the $S_N2(\beta)$ type of reaction cannot be observed experimentally in the gas phase.[3m] The correlated activation energy barriers are lowered ($\delta\Delta E^‡$ (=$\Delta E^‡_{MP} - \Delta E^‡_{RHF}$) < 0) by a greater amount for the reactions of SH^- than for OH^-, suggesting that electron correlation effects in the TS are greater for the reactions with SH^-. The major reason for this trend is again the greater contribution of electron-localized structures in the TS involving SH^-. The MP2 TS structures are presented in Figure 3.

Since SH^- is a weaker gas-phase nucleophile than OH^-, the TSs occur later on the reaction coordinate and exhibit a greater C−Z bond cleavage,[8h] i.e., a larger %CZ‡ value (Table 4). The magnitudes of %CX‡ as well as %CZ‡ values shown in Table 4 are consistent with the bond orders (*n*) at the TS calculated by $n = \exp\{(r^o - r^‡)/0.6\}$,[14] where r^o refers to the bond length of either the reactant or product and $r^‡$ denotes the bond length in the TS. For $S_N2(\alpha)$ reactions, the bond orders of C−Cl at the TS, $n_{(C-Cl)}$, are 0.55 (OH^-) and 0.48 (SH^-), indicating that the bond cleavage of the leaving group Cl is more extensive for the SH^- nucleophile than for the OH^- nucleophile. Thus the results indicate again that the TS for the SH^- nucleophile occurs later on the reaction coordinate compared to that for the OH^- nucleophile.

The secondary kinetic isotope effects (SKIEs), k_H/k_D, determined with the substrate deuterated at the β-carbon, $NCCD_2$-CH_2Cl, are summarized in Table 5. Quantum mechanical tunneling effects influence the magnitude of the isotope effect, but the tunneling influences mainly primary effects.[15] Thus we neglected the tunneling effect. All the k_H/k_D values are less than unity, indicating an increase in the vibrational frequencies due to steric crowding in the TS,[16] and they are smaller for $S_N2(\beta)$ than for the $S_N2(\alpha)$. This is reasonable since steric crowding effects will be greater in the former, an α-deuterium KIE, compared to the KIEs for the latter, a β-deuterium KIE.[16] Although β-deuterium KIEs are normal type, $k_H/k_D > 1.0$, in most cases,[17] the values in Table 5 are inverse type, $k_H/k_D < 1.0$, due most probably to the strong steric crowding effect in the TS. Since the TSs for the SH^- reactions are looser than those for the OH^- (Table 4), the steric crowding will be less so that the k_H/k_D values are larger for SH^-.

On the other hand, the $\Delta E^‡$ values for the reactions of **II** (Table 3) indicate that substitution of a strong electron-withdrawing group, CN, for a β-hydrogen leads to lowering of the barrier heights by 8−10 kcal mol^{-1} at the MP2 level as predicted in the above electron-localized configuration, **III**. The lowering effect of barrier height by the CN substituent is consistent with the previously reported works[3p,7n] for the S_N2 reactions.

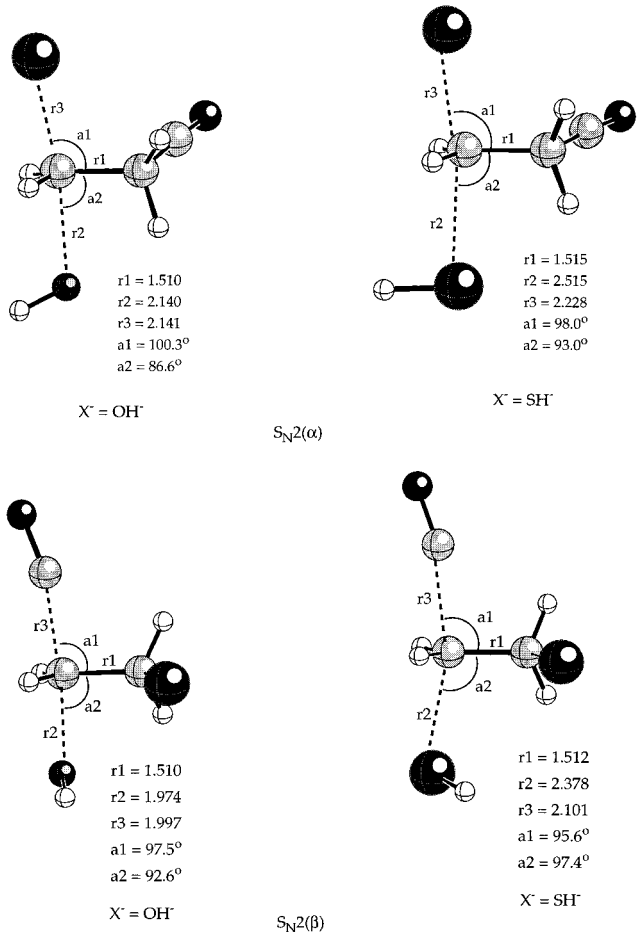

Figure 3. S_N2 TS structure at the MP2 level.

TABLE 5: Calculated Secondary KIE for the S_N2 Reactions

X^-	path	level	k_H/k_D
OH^-	$S_N2(\alpha)$	RHF	0.962
		MP2	0.856
	$S_N2(\beta)$	RHF	0.867
		MP2	0.796
SH^-	$S_N2(\alpha)$	RHF	0.993
		MP2	0.958
	$S_N2(\beta)$	RHF	0.903
		MP2	0.944

Elimination Reactions. Two possible pathways for the elimination reactions are formations of cyanoethene initiated by deprotonation of a β-hydrogen (β-H-elim.) and of chloroethene induced by deprotonation of an α-hydrogen (α-H-elim.), Scheme 1. However, in the α-H-elimination both the energies of activation, $\Delta E^‡$, and reaction, $\Delta E°$, are expected to be prohibitively high due to the poor leaving ability of CN^-, as we have discussed above for the $S_N2(\beta)$ reaction. We have therefore attempted calculations of the potential energy surface for the α-H-elimination involving the strong nucleophile, OH^-, only. The first step was deprotonation of an α-hydrogen leading to an anionic intermediate. The activation energy ($\Delta E_1^‡$) at the MP2 level was low, with −21.27 kcal mol^{-1} for the deprotonation step. The second step involves departure of the leaving group, CN^-, forming chloroethene product. For this step the activation barrier ($\Delta E_2^‡$) was much higher, −3.77 kcal mol^{-1}.

TABLE 6: Calculated Activation Energies ($\Delta E^{\ddagger}$ and $\Delta E_0^{\ddagger}$), Complexation Energies (ΔE_{RC} and ΔE_{PC}), and Reaction Energies (ΔE° and ΔE_0°) for the E2 Reaction Paths in kcal mol^{-1}

X$^-$	path	level	$\Delta E^{\ddagger}$	$\Delta E_0^{\ddagger}$	ΔE_{RC}	ΔE_{PC}	ΔE°	ΔE_0°
OH$^-$	(A)[a]	RHF	−26.32 (−3.36)[c]	3.85	−30.17	−25.48	−56.07	−51.39
		MP2	−32.00 (−8.66)[c]	0.58	−32.57	−31.48	−38.26	−37.16
	(G)[b]	RHF	−20.56	9.61	−30.17	−25.48	−56.07	−51.39
		MP2	−26.95	5.62	−32.57	−31.48	−38.26	−37.16
SH$^-$	(A)[a]	RHF	11.82 (28.29)[c]	28.41	−16.59	−20.98	−5.82	−10.21
		MP2	−3.89 (18.80)[c]	16.82	−20.71	−26.93	−0.08	−6.30
	(G)[b]	RHF	18.88	35.47	−16.59	−20.98	−5.82	−10.21
		MP2	2.91	23.63	−20.71	−26.93	−0.08	−6.30

[a] Path via antiperiplanar TS structure. [b] Path via gauche TS structure. [c] Values in parentheses are the activation energies for reactions of CH_3CH_2Cl with X$^-$.

SCHEME 4

The overall reaction energy was −5.08 kcal mol^{-1}. The α-H-elimination with OH$^-$ proceeds therefore through two steps, an E1cb reversible mechanism.[17] Although $\Delta E^{\ddagger}$ and ΔE° are negative, they are much less negative (and hence much more unfavorable) than those corresponding values for the *β*-H-elimination with OH$^-$ in Table 6. Thus, the α-H-elimination pathway leading to the chloroethene product is highly unfavorable kinetically and thermodynamically compared to the *β*-H-elimination leading to the cyanoethene product. Reference to Table 6 reveals that the activation energies for the *β*-H-elimination of CH_3CH_2Cl, **II**, are much higher, by ca. 23 kcal mol^{-1}, than those for the *β*-H-elimination of **I**. In view of the near central E2 TS structure reported for the *β*-H-elimination of **II**,[8d] the *β*-H-elimination of **I** is likely to proceed by an E1cb-like TS.[18] To examine the TS structure variation by a CN substituent, we calculated the deprotonated anion intermediate of *β*-hydrogen for 2,2-dicyanoethyl chloride, $(NC)_2CHCH_2Cl$, at both the RHF and MP2/6-31+G* levels. Indeed, we found that the anion intermediate was existent in a stable equilibrium species which is the intermediate of the E1cb mechanism. Thus we expect that the *β*-H-elimination paths of **I** may be *borderline* cases between central E2 and E1cb reaction paths.

Structurally, substitution of a CN group for a *β*-hydrogen, **II** → **I**, makes *β*-hydrogens more acidic, i.e., more positively charged ($\Delta q_{\beta-H} = q_{\mathbf{I}} - q_{\mathbf{II}} = 0.05e$) by 0.05 electronic charge unit (MP2 Mülliken charge) and depresses $\sigma^*_{C\beta-H}$ by ca. 0.04 hartree.

This means that compared to **II** deprotonation of a *β*-hydrogen from **I** becomes much more facilitated. Thus the E2 processes are predominant over the S_N2 processes in the reactions of **I**, whereas the S_N2 processes are more favorable compared to the E2 processes in the reactions of **II** (Tables 3 and 6).

E2 Transition States. Examination of the reactant complexes, RC3, in Figure 2, shows that deprotonation of either of the two *β*-hydrogens, at anti and gauche with respect to the C_α−Cl bond, is equivalent. Therefore both anti and gauche eliminations must be considered in search of the TS structure. Characterization of the E2 TS structure was rather involved, since in the E2 elimination reaction proton transfer, leaving group departure, and double-bond formation occur concertedly and identification of a normal mode corresponding to an imaginary vibration frequency is not an easy task. Comparison of the activation barriers ($\Delta E^{\ddagger}$) in Tables 3 and 6 indicates that the E2 reactions are preferred to the S_N2 reactions of **I** with both OH$^-$ and SH$^-$ and Cl$^-$ as the leaving group.

SCHEME 5

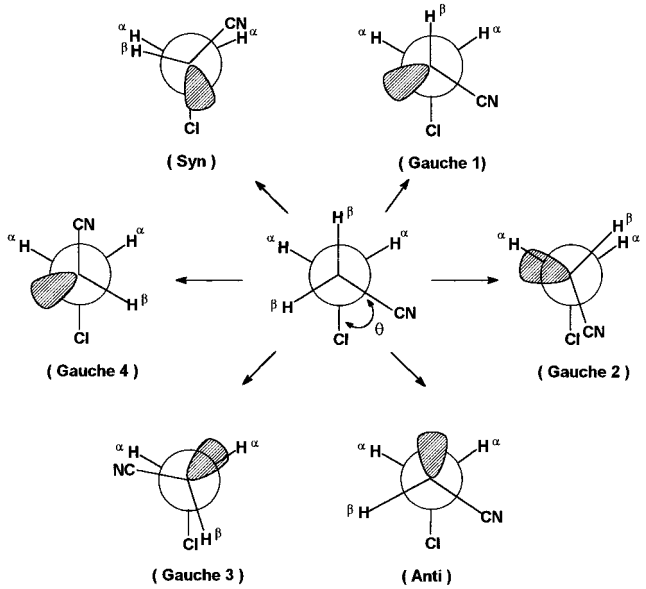

Possible TS structures for elimination reactions via stable RC3.

TABLE 7: Calculated TS Energies of the Various Elimination Paths at the RHF/6-31+G* Level in Hartrees

X$^-$	gauche 1	gauche 4	anti
OH$^-$	−705.274 23	−705.274 35	−705.283 42
SH$^-$	−1027.941 85	−1027.942 26	−1027.953 12

The OH$^-$ base is a strong thermodynamic as well as kinetic base, as evidenced by large exothermicities of the reaction and by large negative activation barriers (Table 6) for both anti and gauche eliminations of **I**. However, SH$^-$ is a much weaker base than OH$^-$ so that the anti and gauche *β*-H-eliminations of **I** with SH$^-$ are nearly thermoneutral ($\Delta E^{\circ}_{MP} = -0.1$ kcal mol^{-1}). The $\Delta E^{\ddagger}$ for the gauche elimination with SH$^-$ is positive ($\Delta E^{\ddagger}_{RHF} = 18.9$ and $E^{\ddagger}_{MP} = 2.9$ kcal mol^{-1}), and hence the gauche pathway is much more unfavorable than the anti one ($\delta\Delta E^{\ddagger}_{MP} \cong 6.8$ kcal mol^{-1}). In general, the anti is preferred to the gauche elimination since a relatively strong n−σ^* interaction[19] between the developing lone pair on $C_\beta(n)$ and the σ^*_{C-Cl} orbital renders an additional stabilization to the antiperiplanar E2 TS.

Reference to Table 6 reveals that inclusion of electron correlation effects results in depression of the activation energies for the *β*-H-eliminations much more with SH$^-$ ($\delta\Delta E^{\ddagger} = E^{\ddagger}_{MP} - E^{\ddagger}_{RHF} \cong -15$ kcal mol^{-1}) than with OH$^-$ ($\delta\Delta E^{\ddagger} = -6$ kcal mol^{-1}), which is in contrast to a much greater elevation of reaction energies ($\delta\Delta E^{\circ} = \Delta E^{\circ}_{MP} - \Delta E^{\circ}_{RHF} \cong +16$ kcal mol^{-1}) for OH$^-$ compared to that ($\delta\Delta E^{\circ} = +6$ kcal mol^{-1}) for SH$^-$.

There are several structures conceivable for the TSs depending on the stereochemical orientation of the developing lone pair upon deprotonatoin of a *β*-hydrogen, as shown in Scheme 5. The RHF/6-31+G* energies are calculated for the three most probable structures as listed in Table 7. Among the structures shown in Scheme 5, the syn type TS structure was nonexistent and was found to be a transient rotamer on the path toward the gauche 4 form, and the gauche 2 structure corresponded to a

transient rotamer on the path toward the anti form. These two transient forms are unstable because of strong electronic repulsions between two eclipsed pairs, n····Cl and CN····Cl in syn and gauche 2, respectively. On the other hand, the gauche 3 structure with OH^- base had two imaginary frequencies (1305.9i and 68.8i cm^{-1}), disqualifying it as a TS structure. The first imaginary frequency (1305.9i) corresponds to a normal mode of C_β−H stretching, whereas the second one (68.8i) corresponds to a rotational mode around C_α−C_β leading to the most stable rotamer, the anti form. For the β-H-eliminations with SH^-, the gauche 3 form was found to be a transient rotamer leading to the anti form. Consequently, there are three TS structures left, anti, gauche 1, and gauche 4, as stationary point species. Of the two gauche forms, gauche 1 and 4, repulsive interaction between CN and Cl is relatively weaker in gauche 4 than in gauche 1 due to the longer distance between them. As a result, gauche 4 is more stable than gauche 1. However the energy difference between gauche 1 and gauche 4 is very small (Table 8) and gauche 4 is formed by rotation around C_α−C_β. Thus the gauche 1 may be more reasonable than gauche 4 by adopting the principle of least motion.[20] We therefore excluded the syn and gauche 2−4 forms from our subsequent discussions. The anti and gauche 1 TS structures are presented in Figure 4, and structural changes for the two TSs are summarized in Table 8. We note that deprotonation is considerably ahead of leaving group departure and C_α=C_β double-bond formation in general, indicating an E1cb-like TS structure (Table 8). Moreover, deprotonation has progressed to a greater extent in E2 (gauche 1) for OH^- (Figure 4), but other structural reorganizations, leaving group departure and contraction of the C_α−C_β bond, have progressed to a greater extent in anti. The latter, more progressed structural changes in anti are, of course, due to the optimum stereochemical arrangement of the lone pair (n) vs the C−Cl bond for the strong n−σ_{C-Cl} interaction,[19] leading to a facile C−Cl bond cleavage (an antiperiplanar form). For example, the dihedral angle, $\theta = \angle ClC_\alpha C_\beta H$, is almost an ideal

TABLE 8: Structural Changes in the TSs

		anti TS		gauche 1 TS	
X^-	$\%\Delta d^{\ddagger}$ [a]	RHF	MP2	RHF	MP2
OH^-	C−Cl	3.9	2.7	1.8	1.3
	C_β−H	16.6	12.0	17.3	14.7
	C_α−C_β	14.4	14.8	5.6	7.7
	θ [b]	170.7	171.8	63.5	67.2
SH^-	C−Cl	8.7	9.7	4.7	6.8
	C_β−H	51.1	54.1	52.0	46.4
	C_α−C_β	32.5	44.3	17.8	30.8
	θ [b]	169.4	172.2	46.7	19.6

[a] $\%\Delta d^{\ddagger} = [(d_{TS} - d_R)/(d_P - d_R)] \times 100$. [b] θ denotes $\angle ClC_\alpha C_\beta H$ in degrees.

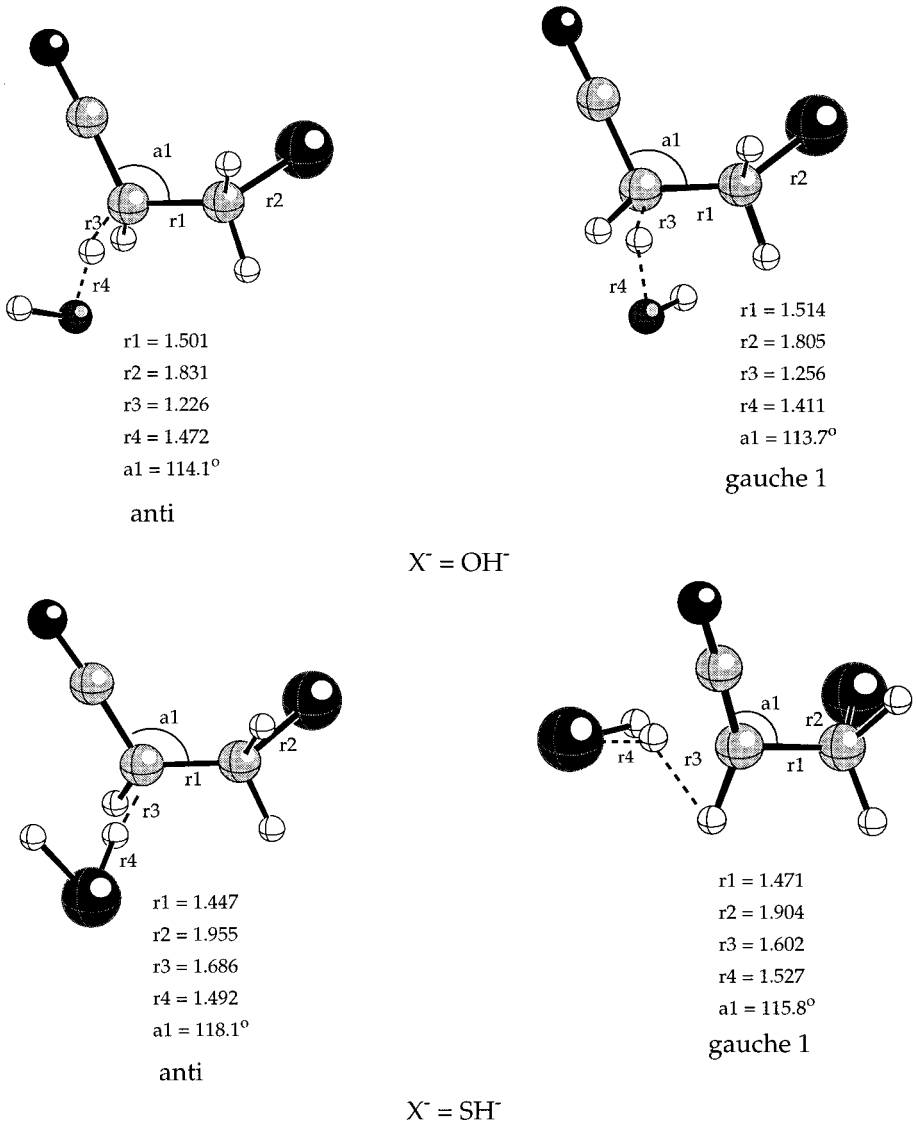

Figure 4. Elimination (anti and gauche 1) TS structure at the MP2 level.

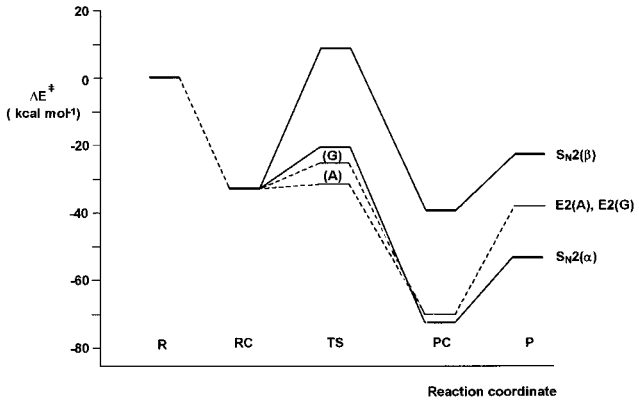

Figure 5. Potential energy surfaces for the reaction with OH^- at the MP2 level.

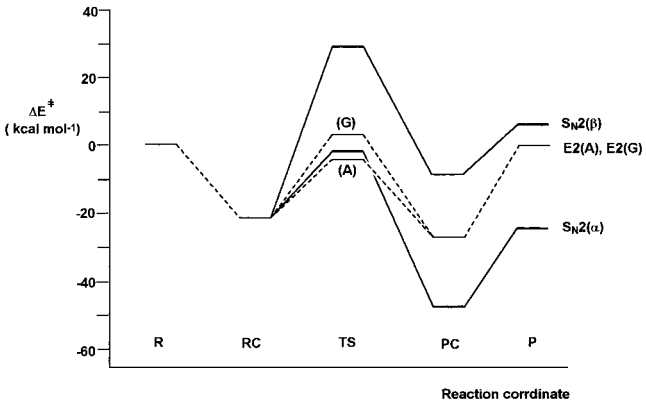

Figure 6. Potential energy surfaces for the reaction with SH^- at the MP2 level.

antiperiplanar value of 180° (172°) in the anti form, whereas it is only 67° (OH^-) and 20° (SH^-) in the gauche 1 form. For both OH^- and SH^-, deprotonation of a β-hydrogen has progressed to a greater extent than leaving group departure and double-bond formation, indicating that the elimination proceeds by an E1cb-like E2 mechanism. Another notable feature in Table 8 is that the β-H-elimination with SH^- has progressed further along the reaction coordinate compared to that with OH^-.

The difference in the thermodynamic basicity between OH^- and SH^- is not the only cause of the large differences in the kinetic barriers, $\delta\Delta E^{\ddagger}_{MP}$ ($=\Delta E^{\ddagger}_{SH^-} - \Delta E^{\ddagger}_{OH^-}$) of +28 to +29 kcal mol^{-1} for the β-H-elimination reactions of **I** and **II** (Table 6) and $\delta\Delta E^{\ddagger}_{MP}$ of +17 to +19 kcal mol^{-1} for the S_N2 processes of **I** and **II** (Table 3). For the reactions of **II** with F^- and PH_2^- which have the same thermodynamic basicities,[8d] the kinetic reactivities ($\delta\Delta E^{\ddagger}$) were very different. With PH_2^-, the activation barriers for S_N2 and E2 reactions were both larger than those found with F^-. This means that there is a larger kinetic barrier for PH_2^- to form new bonds to carbon and hydrogen. This has been ascribed to the greater electronic reorganization required for the S_N2 and E2 processes with PH_2^-.[8d] Second-row elements such as P and S form bonds to C and H with most of the shared electron density polarized away from the P or S. Thus a reversal in polarity must take place since generally the nucleophilic site in a base is more electronegative than the atom it attacks (C or H). This reversal of polarity required for the second-row nucleophiles in S_N2 and E2 reactions causes greater electronic reorganizations and as a result leads to larger activation barriers.

S_N2 vs E2. The greater activation energy differences, $\delta\Delta E^{\ddagger}_{MP}$ ($=\Delta E^{\ddagger}_{SH^-} - \Delta E^{\ddagger}_{OH^-}$) $\cong$ 28−29 kcal mol^{-1} in the E2 reactions (Table 6) than those, $\delta\Delta E^{\ddagger}_{MP} \cong$ 17−19 kcal mol^{-1}, in the S_N2 reactions (Table 3) for the reactions of **I** and **II** reflect correctly the gas-phase experimental results of preferential E2 reaction for first-row, strongly basic localized anions containing F, N, or O at the nucleophilic center in contrast to the preference of S_N2 reaction for second-row and/or delocalized anions.[3m,n,4b] This trend is consistent with the notion that sulfur anions are better nucleophiles than bases.[3m,n,4b]

The potential energy surfaces based on the MP2/6-31+G* activation energies, $\Delta E^{\ddagger}$, are presented in Figures 5 and 6. For both anionic bases, OH^- and SH^-, the E2(A) pathway is the most preferred and the $S_N2(\beta)$ path is the least preferred. The $S_N2(\alpha)$ path becomes competitive with the E2(A) path for SH^-, which is again a reflection of preferential S_N2 reaction for second-row, weakly basic anions. The reactions with OH^- are far more exothermic than those with SH^- due to the strong basicity of the OH^- ion in the gas phase. To examine the effects of electron correlation on the relative barrier heights, we extended our calculations of the activation barriers, $\Delta E^{\ddagger}$, to the MP3, MP4D, MP4DQ, and MP4SDQ levels.[10] For higher level MP calculations, up to MP4SDQ, of $\Delta E^{\ddagger}$, single-point calculations were carried out with the MP2/6-31+G* geometries.[10] The results are summarized in Table 9.

We note that there is no reversal in the relative order of barrier heights, $\Delta E^{\ddagger}$, for OH^-. In contrast, there is a reversal from preferential E2(A) at the MP2 level to preferential $S_N2(\alpha)$ at the higher MP levels for SH^-, although the difference in the barrier height between the two lowest reaction pathways is small. There is very little change in the $\Delta E°$ values at the successively higher order MP levels.

Conclusion

The S_N2 and E2(anti) reactions of OH^- and SH^- with $NCCH_2CH_2Cl$ are exothermic and have negative activation

TABLE 9: Calculated Activation Energies ($\Delta E^{\ddagger}$) and Reaction Energies ($\Delta E°$) at the Higher Levels of Electron Correlation Effect in kcal mol^{-1}

X^-	path		RHF	MP2	MP3	MP4D	MP4DQ	MP4SDQ
OH^-	E2(A)	$\Delta E^{\ddagger}$	−26.32	−32.00	−31.18	−30.67	−29.78	−30.24
	E2(G)	$\Delta E^{\ddagger}$	−20.56	−26.95	−26.00	−25.58	−24.59	−24.96
		$\Delta E°$	−56.07	−38.26	−43.32	−42.14	−41.50	−40.22
	$S_N2(\alpha)$	$\Delta E^{\ddagger}$	−21.22	−21.14	−20.17	−20.01	−19.15	−21.43
		$\Delta E°$	−72.67	−53.83	−59.24	−57.41	−57.34	−55.94
	$S_N2(\beta)$	$\Delta E^{\ddagger}$	11.77	9.66	9.92	9.58	10.76	8.47
		$\Delta E°$	−36.58	−23.20	−29.44	−27.96	−27.62	−26.70
SH^-	E2(A)	$\Delta E^{\ddagger}$	11.82	−3.89	−0.12	−0.46	1.08	0.01
	E2(G)	$\Delta E^{\ddagger}$	18.88	2.91	6.31	6.13	7.61	6.71
		$\Delta E°$	−5.82	−0.08	−0.85	−1.56	−1.13	−1.32
	$S_N2(\alpha)$	$\Delta E^{\ddagger}$	2.30	−2.54	−0.72	−0.67	−0.18	−2.01
		$\Delta E°$	−24.12	−24.12	−23.97	−23.79	−23.87	−23.77
	$S_N2(\beta)$	$\Delta E^{\ddagger}$	38.19	29.04	30.77	30.08	31.19	28.88
		$\Delta E°$	11.68	6.52	5.82	5.71	5.84	5.51

energies when Cl^- is the leaving group, and both pathways are viable under typical gas-phase reaction conditions, although E2 is preferred to S_N2 overall. In both cases, however, the reactions of OH^- are highly favored, but the E2(anti) reaction of SH^- is the least favored. This is in contrast to the reactions of PH_2^- with CH_3CH_2Cl; PH_2^- is capable of only a slow S_N2 reaction and canot induce an elimination reaction, although the proton affinity (PA) of PH_2^- (370.9 ± 2.0 kacl mol^{-1}) is greater than that of SH^- (351.0 kcal mol^{-1}). Obviously, substitution of a CN group for a β-hydrogen facilitates both the S_N2 and E2 processes compared to those of CH_3CH_2Cl and makes the E2 path become more E1cb-like. The E2(anti) is significantly favored over the E2(gauche) for both OH^- and SH^-, indicating that an antiperiplanar TS is preferred in the gas phase. In all cases, the reaction of SH^- base has a later TS along the reaction coordinate and a higher activation barrier compared to that of OH^-. This is due not only to the lower thermodynamic basicity (lower PA leading to lower exothermicity) but also to the lower kinetic basicity (reversal in bond polarity in the TS leading to greater electronic reorganization) of second-row nucleophiles.

Acknowledgment. We thank the Ministry of Education of Korea (BSRI-96-3428) and Inha University for support of this work.

References and Notes

(1) (a) Lower, T. H.; Richardson, K. S. *Mechanism and Theory in Organic Chemistry*, 3rd ed.; Harper and Row: New York, 1987; Chapters 4 and 7. (b) Jones, R. A. Y. *Physical and Mechanistic Organic Chemistry*; Cambridge University Press: Cambridge, 1979; Part 2. (c) Shaik, S. S.; Schlegel, H. B.; Wolfe, S. *Theoretical Aspects of Physical Organic Chemistry. The S_N2 Mechanism*; Wiley: New York, 1992; Chapters 4−6. (d) Pross, A. *Theoretical and Physical Principles of Organic Reactivity*; Wiley: New York, 1995: Part C. (e) Harris, J. M., McManus, S. P., Eds. *Nucleophilicity*; Advances in Chemistry Series 215; American Chemical Society: Washington, DC, 1987. (f) Ingold, C. K. *Structure and Mechanism in Organic Chemistry*; Cornell University Press: Ithaca; New York, 1969. (g) Isaacs, N. S. *Physical Organic Chemistry*; Longman: Harlow, 1987; Chapters 10 and 11.

(2) (a) Bartsch, R. A.; Zavada, *J. Chem. Rev.* **1980**, *80*, 454. (b) Saunders, W. H., Jr.; Cockerill, A. F. *Mechanism of Elimination Reactions*; Wiley: New York, 1973.

(3) (a) Bohme, D. K.; Mackay, G. I.; Payzant, J. D. *J. Am. Chem. Soc*. **1974**, *96*, 4027. (b) Payzant, J. D.; Tanaka, K.; Betowski, L. D.; Bohme, D. K. *J. Am. Chem Soc*. **1976**, *98*, 894. (c) Bohme, D. K. In *Ionic Processes in the Gas Phase*; Ferreira, M. A., Ed.; Reidel: Dordrecht, 1984; Part 111. (d) Riveros, J. M.; José, S. M.; Takashima, K. *Adv. Phys. Org. Chem*. **1985**, *21*, 197. (e) Brauman, J. I.; Olmstead, W. N.; Lieder, C. A. *J. Am. Chem. Soc*. **1974**, *96*, 4030. (f) Olmstead, W. N.; Brauman, J. I. *J. Am. Chem. Soc*. **1977**, *99*, 4219 (g) Pellerite, M. J.; Brauman, J. I. *J. Am. Chem. Soc*. **1980**, *102*, 5993 (h) Pellerite, M. J.; Brauman, J. I. *J. Am. Chem. Soc*. **1983**, *105*, 2672. (i) Han, C.-C.; Dodd, J. A. Pellerite, M.; Brauman, J. I. *J. Phys. Chem*. **1986**, *90*, 471. (j) Dodd, J. A.; Brauman, J. I. *J. Phys. Chem*. **1986**, *90*, 3559. (k) Barlow, S. E.; Van Doren, J. M.; Bierbaum, V. M. *J. Am. Chem. Soc*. **1988**, *110*, 7240. (l) Caldwell, G.; Magnera, T. F.; Kebarle, P. *J. Am. Chem. Soc*. **1984**, *106*, 959. (m) Depuy, C. H.; Gronert, S.; Mullin, A.; Bierbaum, V. M. *J. Am. Chem. Soc*. **1990**, *112*, 8650. (n) Gronert, S.; Depuy, C. H.; Bierbaum, V. M. *J. Am. Chem. Soc*. **1991**, *113*, 4009. (o) Wilbur, J. L.; Brauman, J. I. *J. Am. Chem. Soc*. **1991**, *113*, 9699. (p) Wladkowskii, B. D.; Lim, K. F.; Allen, W. D.; Brauman, J. I. *J. Am. Chem. Soc*. **1992**, *114*, 9136. (q) Wladkowskii, B. D.; Wilbur, J. L.; Brauman, J. I. *J. Am. Chem. Soc*. **1994**, *116*, 2471. (r) Wladkowskii, B. D.; Brauman, J. I. *J. Phys. Chem.* **1993**, *97*, 13158. (s) Born, M.; Ingemann, S.; Nibbering, N. M. M. *J. Chem. Soc., Perkin Trans. 2* **1996**, 2537.

(4) (a) Jones, M. E.; Ellison, G. B. *J. Am. Chem. Soc*. **1989**, *111*, 1645. (b) Lum, R. C.; Grabowski, J. J. *J. Am. Chem. Soc*. **1992**, *114*, 9663.

(5) (a) Asubiojo, O. I.; Brauman, J. I. *J. Am. Chem. Soc*. **1979**, *101*, 3715. (b) Kim, J. K; Caserio, M. C. *J. Am. Chem. Soc*. **1981**, *103*, 2124. (c) Bartmess, J. E.; Hays, R. L.; Caldwell, G. *J. Am. Chem. Soc*. **1981**, *103*, 1338. (d) Baer, S.; Brinkman, E. A.; Brauman, J. I. *J. Am. Chem. Soc*. **1991**, *113*, 805. (e) Wilbur, J. L.; Brauman, J. I. *J. Am. Chem. Soc*. **1994**, *116*, 5839. (f) Wilbur, J. L.; Brauman, J. I. *J. Am. Chem. Soc*. **1994**, *116*, 9216. (g) McDonald, R. N.; Chowdhury, A. K. *J. Am. Chem. Soc*. **1983**, *105*, 198. (h) McDonald, R. N.; Chowdhury, A. K. *J. Am. Chem. Soc*. **1983**, *105*, 7267. (i) McDonald, R. N.; Chowdhury, A. K. *J. Am. Chem. Soc*. **1985**, *107*, 4123.

(6) Wolfe, S.; Mitchell, D. J.; Schlegel, H. B. *J. Am. Chem. Soc*. **1981**, *103*, 7694.

(7) (a) Shi, Z.; Boyd, R. J. *J. Am. Chem. Soc*. **1990**, *112*, 6789. (b) Shi, Z.; Boyd, R. J. *J. Am. Chem. Soc*. **1991**, *113*, 1072. (c) Boyd, R. J.; Kim, C. K.; Shi, Z.; Weinberg, N.; Wolfe, S. *J. Am. Chem. Soc*. **1993**, *115*, 10147. (d) Zhao, X. G.; Tucker, S. C.; Truhlar, D. G. *J. Am. Chem. Soc*. **1994**, *116*, 7797. (e) Wladkowskii, B. D.; Allen, W. D.; Brauman, J. I. *J. Phys. Chem.* **1994**, *98*, 13532. (f) Harder, S.; Streitwieser, A.; Petty, J. T.; Schleyer, P. v. R. *J. Am. Chem. Soc*. **1995**, *117*, 3253. (g) Deng, L.; Branchadell, V.; Ziegler, T. *J. Am. Chem. Soc*. **1994**, *116*, 10645. (h) Glukhovtsev, M. N.; Pross, A.; Radom, L. *J. Am. Chem. Soc*. **1995**, *117*, 9012. (i) Glukhovtsev, M. N.; Pross, A.; Schlegel, H. B.; Bach, R. D.; Radom, L. *J. Am. Chem. Soc*. **1996**, *118*, 11258. (j) Vetter, R.; Zülike, L. *J. Am. Chem. Soc*. **1990**, *112*, 5136. (k) Lee, I.; Kim, C. K.; Chung, D. S.; Lee, B.-S. *J. Org. Chem.* **1994**, *59*, 4490. (l) Park, Y. S.; Kim, C. K.; Lee, B.-S.; Lee, I. *J. Phys. Chem.* **1995**, *99*, 13103. (m) Lee, I.; Kim, C. K.; Lee, B.-S. *J. Phys. Org. Chem.* **1995**, *8*, 473. (n) Lee, I.; Kim, C. K.; Lee, B.-S. *J. Comput. Chem.* **1995**, *16*, 1045.

(8) (a) Minato, T.; Yamabe, S. *J. Am. Chem. Soc*. **1988**, *110*, 4586. (b) Minato, T.; Yamabe, S. *J. Am. Chem. Soc*. **1985**, *107*, 4621. (c) Pross, A.; Shaik, S. S. *J. Am. Chem. Soc*. **1982**, *104*, 187. (d) Gronert, S. *J. Am. Chem. Soc*. **1991**, *113*, 6041. (e) Gronert, S. *J. Am. Chem. Soc*. **1992**, *114*, 2349. (f) Gronert, S. *J. Am. Chem. Soc*. **1993**, *115*, 652. (g) Gronert, S. *J. Org. Chem.* **1994**, *59*, 7046. (h) Gronert, S.; Lee, J. M. *J. Org. Chem.* **1995**, *60*, 4488.

(9) Frisch, M. J.; Trucks, G. W.; Head-Gordon, M.; Gill, P. M. W.; Wong, M. W.; Foresman, J. B.; Johnson, B. G.; Schelgel, H. B.; Robb, M. A.; Replogle, E. S.; Gomperts, R.; Andres, J. L.; K.; Raghavachari, J.; Binkley, S.; Gonzalez, C.; Martin, R. L.; Fox, D. J.; Defrees, D. J.; Baker, J.; Stewart, J. J. P.; Pople, J. A. *Gaussian 92, Revision C*; Gaussian Inc.: Pittsburgh, PA, 1992.

(10) Hehre, W. J.; Radom, L. Schleyer, P. v. R.; Pople, J. A. *Ab Initio Molecular Orbital Theory*; Wiley: New York, 1986; Chapter 4.

(11) Schlegel, H. B. In *Ab Initio Methods in Quantum Chemistry, Part 1*; Lawley, K. P., Ed.; Wiley: Chichester, 1987; pp 249−286.

(12) Carey, F. A.; Sundberg, R. J. *Advanced Organic Chemistry, Part A*, 3rd ed.; Plenum Press: New York, 1990; Chapter 3.

(13) (a) Lee, I.; Kim, C. K.; Lee, B.-S. *J. Phys. Org. Chem* **1995**, *8*, 473.

(14) Houk, K. N.; Gustavson, S. M.; Black, K. A. *J. Am. Chem. Soc*. **1992**, *114*, 8565.

(15) (a) Buncel, E., Lee, C. C., Eds. *Isotopes in Organic Chemistry*; Elsevier: Amsterdam, 1976; Vol. 2. (b) Bell, R. P. *The Tunnel Effect in Chemistry*; Chapman and Hall: London, 1980. (c) Garrett, B. C.; Truhlar, D. G. *J. Am. Chem. Soc*. **1980**, *102*, 2559. (d) Kreevoy, M. M.; Ostvic, D.; Truhlar, D. G.; Garrett, B. C. *J. Phys. Chem*. **1986**, *90*, 3766. (e) Glad, S. S.; Jensen, F. *J. Chem. Soc., Perkin Trans. 2* **1994**, 871.

(16) (a) Poirier, R. A.; Wang, Y.; Westaway, K. C. *J. Am. Chem. Soc*. **1994**, *116*, 2526. (b) Lee, I. *Chem. Soc. Rev.* **1995**, *24*, 223. (c) Glad, S. S.; Jensen, F. *J. Am. Chem. Soc*. **1997**, *119*, 227.

(17) (a) Melander, L.; Saunders, W. H. *Reaction Rates of Isotopic Molecules*; Wiley: New York, 1980. (b) Lowry, T. H.; Richardson, K. S. *Mechanism and Theory in Organic Chemistry*, 3rd ed.; Harper and Row: New York, 1987; p 232.

(18) Reference 16b; Chapter 7.

(19) (a) Epiotis, N. D.; Cherry, W. R.; Shaik, S. S.; Yates, R. L.; Bernardi, F. *Structural Theory of Organic Chemistry*; Springer-Verlag: Berlin, 1977. (b) Lee, I.; Chun, Y. G.; Yang, K. *J. Comput. Chem*. **1982**, *3*, 565.

(20) Rice, F. O.; Teller, E. *J. Chem. Phys*. **1938**, *6*, 489; **1939**, *7* 199.